Comparison of Measurement and Calculation of the Electric Field Transfer Function for an Active Implant Lead in Different Media

John Nyenhuis[1], John Jallal[2], Xiaoyi Min[2], Shiloh Sison[2], Gabriel Mouchawar[2]

[1]Purdue University, West Lafayette, USA
[2]St Jude Medical Inc., Sylmar, USA

Abstract

Patients with an active implantable medical device (AIMD) may be at risk of harm from RF-induced heating during an MRI scan. The electric field transfer function (TFE) is a measure of the sensitivity of the heating at the electrode of the AIMD to the incident tangential electric field (Etan) along its length. It is demonstrated that the TFE depends on boundaries of the phantom, phantom media and the trajectory of the AIMD.

For a 60cm simplified straight lead, the measured and simulated TFE in High Permittivity Media (HPM) and Low Permittivity Media (LPM) are compared. TFE for infinite space are simulated and compared to measured TFE. TFE were also measured for different immersion depths and for the lead in U-shape pathway.

For a 1/8-in x 10cm titanium rod, the TFE and temperature rise was measured at multiple immersion depths and at the simulated SAR in the phantom.

The maximum magnitude of TFE for the lead and the Ti rod was reduced by about 8% when the immersion depth was reduced from 7.5 cm to 2 cm. Temperature rises measured on the Ti rod confirm a 15% reduction when the distance from the phantom wall was changed from 7.5cm to 2cm.The shape of the TFE for the lead was measured to be different when the lead was arranged in a U path than when arranged in a straight line path. Differences between TFEs in HPM and LPM arise from the longer wavelength in LPM and the greater attenuation in HPM.

1. Introduction

Patients with active implantable medical devices (AIMD) may be at risk of harm from RF-induced heating during an MRI scan. The AIMD lead picks up RF energy which gives rise to a current along the lead body and electric fields at the electrodes resulting in increased temperature at the electrode/tissue interface. The amount of RF-induced lead heating is mainly attributed to the electric field tangential (Etan) to the lead path, which can be predicted by using an electrical field transfer function (TFE) associated with different media.

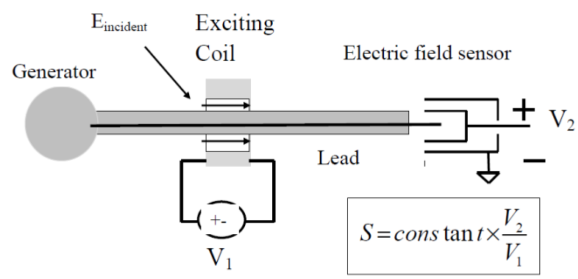

Figure 1. Set up for transfer function measurement.

Tier 3 for RF heating assessment in ISO/TS 10974 [1] requires one to develop an electromagnetic model of the AIMD and demonstrating the equivalence of the model to experimental results.

A method for developing the AIMD lead model is the measurement of the TFE as depicted in Figure 1.[2] The AIMD lead is immersed in liquid phantom media. An incident Etan is produced by applying a voltage V_1 to a suitable transmit antenna, such as the exciting coil indicated in Figure 1. The Etan transmitter induces current waves on the conducting wire of the AIMD. An electric field sensor measures the voltage V_2 that is produced by the current that is transmitted to electrode.

In the measurement, the transfer function S is then proportional to the ratio of the applied and sensed voltages.

$$S \propto \frac{V_2}{V_1} \qquad (1)$$

The temperature rise at the electrode of the lead is then

$$\Delta T = A\left|\int_0^L E_{\tan}(\tau)S(\tau)d\tau\right|^2 \qquad (2)$$

where E_{tan} is the incident tangential electric field, τ is parametric distance along the lead, and A is a scaling constant which can be determined by measurement of the temperature rise in a phantom using a procedure similar to the one described in ASTM F2182-11a. [3].

The AIMD lead model (i.e. S and A) is typically validated by measurement of the temperature rise at the electrode for several lead paths. The lead model is validated if the measured temperature rises differ from the predicted rises in Eq. 2 by less than the combined measurement and model uncertainty.

One origin of uncertainty in the predicted rise for the phantom paths is geometrical. S is impacted by scattering of electric field from the boundaries of the phantom. The transfer function is typically measured in a rectangular phantom with the lead elongated along a straight pathway. The validation is done in a phantom of different geometry, such as the rectangular phantom of ASTM F2182-11a. The predicted rise can also by altered if the scattered field generated by one segment of the lead interacts with a neighboring segment of the lead. Another origin of the uncertainty is the dependence of S and A on the electrical properties of tissues along the length of the lead and the electrical properties of the tissues at the electrode.

One objective of this investigation is to compare the TFE in High Permittivity Media (HPM) and Low Permittivity Media (LPM) for a simplified lead. Another objective is to perform measurements that demonstrate that the TFE depends on boundaries of the phantom and the trajectory of the lead of the AIMD.

1. Materials and methods

Electric field transfer function measurements and simulations were performed on a simplified lead of 60 cm length, 22-gauge wire of diameter 0.7 mm that was covered with insulation with outer diameter of 1.4 mm and $\varepsilon r = 3$ that had an insulating cap at the proximal end and had 3 mm of insulation removed at the distal end to form the electrode. Two media were evaluated: HPM with conductivity $\sigma = 0.47$ S/m and $\varepsilon r = 78$ made from a saline solution and LPM with $\sigma = 0.05$ S/m and $\varepsilon r = 11.5$ (Zurich Med. Tech, Zurich).

HFSS (ANSYS, PA) was used to simulate boundary effects on the TFE. The simplified lead was placed in the center of the phantom and two boundary conditions were simulated: one matched the measurement (Phantom calc) and another with radiation boundary mimicking infinite space ($\propto$ calc).

Boundary effects of the phantom were also tested by measuring the TFE for different immersion depths. The TFE was measured in a straight line for wire immersion depths of 2 cm and 7.5 cm. At immersion depth of 7.5 cm, the transfer function was also measured for the wire in a U path with a separation of 4.5 cm between the sides.

Another model implant used is the 1/8-in x 10 cm titanium rod described in [3]. The TFE was measured as described in [2] with a Bemcalc (W. Lafayette, IN) transfer function system in a phantom with dimension of 15 x 15 x 120 cm. The TFE was measured at immersion depths of 2 cm and 7.5cm. The SAR in the phantom with a Ti rod placed 5cm from the wall was simulated using Bemcalc thermal solver. Temperature rise was measured using Neoptic (Quebec) temperature probes place in holes at the end of the rod for Ti rod placements of 2, 4, 6, and 7.5 cm from the wall of a 42 x 65 x 10 cm ASTM phantom filled with gelled HPM. The phantom was placed in a GE Signa 1.5 T RF coil with RF power of 150 W applied using a sinusoidal continuous-waveform (in CW). The incident B_1 was vertically polarized.

2. Results

Figure 2 and Figure 3 shows TFEs at 64 MHz in HPM and LPM respectively. The TFEs are measured in the phantom, calculated in the phantom and calculated in infinite space. The HPM has the greater dielectric constant and thus greater phase shift over the length of the wire compared to LPM. The difference in TFE for a boundary of the gel 7.5 cm away from the lead and at infinite distance is greater in LPM than in HPM. This could arise from the greater attenuation constant $\alpha = 14.4 m^{-1}$ in HPM compared to $\alpha = 5.16 m^{-1}$ in LPM.

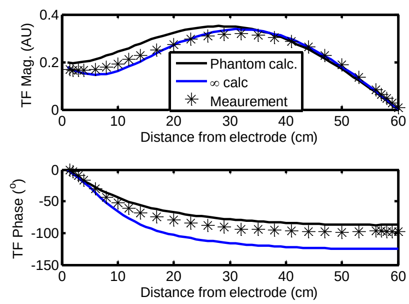

Figure 2. Measured and calculated TFE in HPM.

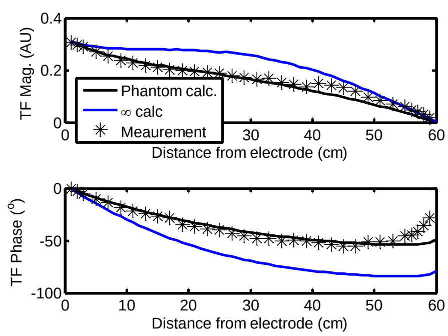

Figure 3. Measured and calculated TFE in LPM.

Figure 4 shows TFE for the 60-cm wire. For the straight line path of the wire, the maximum magnitude of TFE is reduced by 13% for reduction of immersion depth from 7.5 cm to 2 cm. The maximum magnitude of TFE for the U path is 9% greater than maximum magnitude for the straight line path at a depth of 7.5 cm.

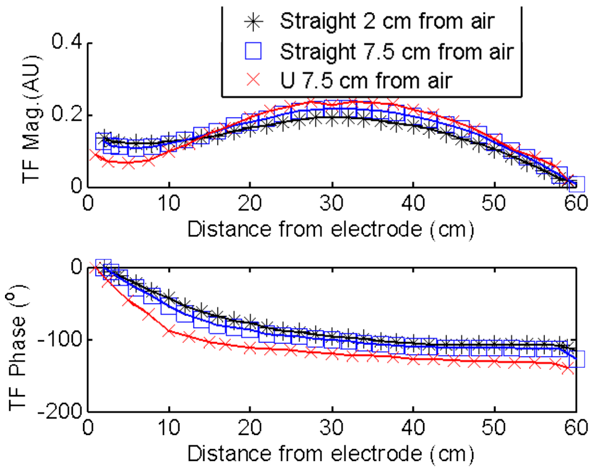

Figure 4. Measured TFE for the 60-cm wire in HPM.

Figure 5 shows the measured TFE for the Ti rod. The maximum magnitude of TFE at the immersion depth of 2 cm is about 7% less than for the immersion depth of 7.5 cm.

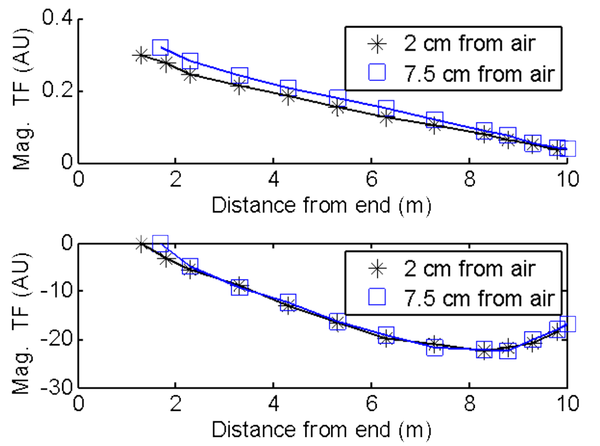

Figure 5. Measured TFE for the 1/8-in diameter x 10 cm long Ti rod in HPM at immersion depth of 2 cm and 7.5cm.

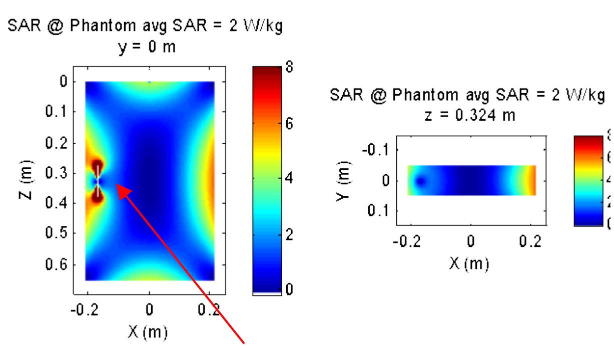

Figure 6. Distribution in ASTM phantom with incident vertical B1 polarized. Ti rod (red arrow) is 5 cm from the wall.

Figure 6 illustrates the mechanism for the boundary effects. The SAR pattern in the ASTM phantom is plotted with a Ti rod at a distance of 5 cm from the wall. There is an increase of SAR at the ends of the rod as expected. There is also increased electric field at the ends of rod due to scattered E field from of the wall of the phantom.

Figure 7 shows the thermal measurement set-up of the Ti rod. The Ti rod is placed on a platform which is placed in contact with the wall of the ASTM phantom. The pegs on the platform are movable such that the distance between the Ti rod and phantom wall can be adjusted. This mimics the positioning shown in Fig. 6. Neoptix temperature probes are seen in the holes at the end of the rod.

Figure 7. Set-up for thermal measurements of Ti rod

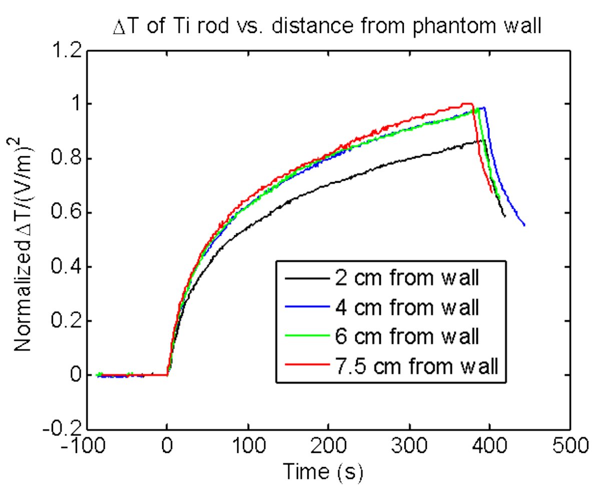

Figure 8 Relative measured temperature rises vs. time at the end of the Ti rod in the ASTM phantom. The rises are scaled to the square of incident Etan and normalized to the rise for the rod at the distance of 7.5 cm from the wall.

Figure 8 shows the temperature rise, normalized to the square of incident Etan, vs. time at the end of the rod. The scaled rise at the distance of 2 cm is about 15% less than the rise at a distance of 7.5 cm. The differences in transfer function are manifested by differences in temperature rises in heating tests in a phantom. Considering the uncertainty, the reduction in the measured rise is consistent with the approximate 7% difference in TFE for immersion depths of 2 and 7.5 cm. (Other factors being the same, temperature rise is proportional to the magnitude of the TFE.)

3. Discussion

The calculations and measurements demonstrate that the transfer function for a lead will depend on the surrounding boundaries and media. The electric field produced by the induced RF current on the lead will be scattered by the boundaries. The scattered electric field will alter the current distribution on the lead. This modification of the incident Etan can be handled by adjusting the Etan in Eq 2 or by altering the effective TFE. This investigation used the effective TFE although either approach may be appropriate.

The boundaries that influence the transfer function may be those of a phantom for in vitro testing. In the patient there will be the boundary of the body surface. Moreover, scattering of the electric field by interfaces between different tissues in the body will influence the transfer function.

The transfer function for a lead is typically measured with the lead in a straight line configuration. However the lead in the patient will not be arrayed in a straight line. TFE is not expected to be influenced much by smooth bends with large radius of curvature. However comparatively tight turns, such as when a section of lead is configured in a loop, or the U path in the validation tests, may produce significant modification of the transfer function.

The visual agreement between the calculated and measured phantom transfer functions in Figs. 2 and 3 demonstrate that the apparatus is capable of accurate measurement of TFE. Thus measurement error in phase and magnitude of TFE are expected to produce a minimal contribution to the uncertainty in the temperature rise as expressed in Eq. 2.

The variation in the transfer function due to scattering from phantom boundaries can result in some differences between the measured temperature rise in a phantom and the temperature rise predicted by Eq. 2. A strategy to improve agreement between measured and calculated rises is to select pathways for validation that are not close to the phantom boundaries.

The measurements and calculations indicate that boundary effects tend to reduce the magnitude of TFE compared to that from radiation boundary conditions. For TFE measurements in phantoms, the lead tends to be at least 6 cm from boundaries. In the patient, a significant length of the lead is sometimes near the surface of the body. Further evaluation is required, but it may be that the in-vivo temperature rise during MRI is overestimated by assuming that the TFE in the patient is the same as the one that is measured in the phantom.

4. Conclusion

Comparison of the calculated and measured TFE for a phantom can be used to assess uncertainty in RF-induced temperature rises. Boundary effects can alter the TFE for an AIMD and should be included in the overall measurement uncertainty. These boundary effects are more pronounced in LPM compared to HPM. Spacing between AIMD segments and between the AIMD and the phantom wall should be considered when designing TFE validation experiments.

References

[1] ISO/TS 10974. ISO/TS 10974, First Edition. Assessment of the safety of magnetic resonance imaging for patients with an active implantable medical device, Reference number ISO/TS 10974:2012(E).

[2] J. Nyenhuis, Using MRI Simulations and Measurements to evaluate RF heating of Active Implants, chapter 21 in MRI Bioeffects, Safety, and Patient Management, edited by F. Shellock and J. Crues, 2014.

[3] ASTM F2182-11a, Standard Test Method for Measurement of Radio Frequency Induced Heating On or Near Passive Implants During Magnetic Resonance Imaging, ASTM International., 2011.

Address for correspondence.

J. Nyenhuis
Purdue University, West Lafayette, IN 47907.
nyenhuis@purdue.edu